The CDK8 inhibitor DCA promotes a tolerogenic chemical immunophenotype in CD4$^+$ T cells via a novel CDK8-GATA3-FOXP3 pathway.

Authors

Azlann Arnett[1], Keagan G Moo[1], Kaitlin J Flynn[1], Thomas B Sundberg[2], Liv Johannessen[3], Alykhan F Shamji[2], Nathanael S Gray[3], Thomas Decker[4], Ye Zheng[5], Vivian H Gersuk[1], David E Levy[6], Isabelle J Marié[6], Ziaur S Rahman[7], Peter S Linsley[1], Ramnik J Xavier[8,9], Bernard Khor[#1]

Affiliations

[1]Benaroya Research Institute, 1201 9th Ave, Seattle, WA 98101, USA.

[2]Center for the Science of Therapeutics, Broad Institute, 415 Main St, Cambridge, MA 02142, USA.

[3]Department of Biological Chemistry and Molecular Pharmacology, Harvard Medical School, 25 Shattuck St, Boston, MA 02115, USA.

[4]Max Perutz Labs, University of Vienna, Dr.-Bohr-Gasse 9, 1030 Wien, Vienna, Austria.

[5]NOMIS Center for Immunobiology and Microbial Pathogenesis, Salk Institute for Biological Studies, 10010 N Torrey Pines Rd, La Jolla, CA 92037, USA.

[6]Department of Pathology, New York University School of Medicine, 550 1st Avenue, New York, NY 10016, USA.

[7]Department of Microbiology and Immunology, Pennsylvania State University College of Medicine, 500 University Drive, Hershey, PA 17033, USA.

[8]Center for Computational and Integrative Biology, Massachusetts General Hospital, Harvard Medical School, 55 Fruit St, Boston, MA 02114, USA.

[9]The Broad Institute of Massachusetts Institute of Technology and Harvard, 415 Main St, Cambridge, MA 02142, USA.

Running Head: T cell differentiation regulated by CDK8-GATA3-FOXP3

#Address correspondence to Bernard Khor, bkhor@benaroyaresearch.org

Word count: Abstract (156); Introduction, Results, and Discussion (3,753); Methods (2,554)

Abstract

Immune health requires innate and adaptive immune cells to engage precisely balanced pro- and anti-inflammatory forces. We employ the concept of chemical immunophenotypes to classify small molecules functionally or mechanistically according to their patterns of effects on primary innate and adaptive immune cells. The high-specificity, low-toxicity cyclin dependent kinase 8 (CDK8) inhibitor DCA exerts a distinct tolerogenic profile in both innate and adaptive immune cells. DCA promotes T_{reg} and Th2 differentiation, while inhibiting Th1 and Th17 differentiation, in both murine and human cells. This unique chemical immunophenotype led to mechanistic studies showing that DCA promotes T_{reg} differentiation in part by regulating a previously undescribed CDK8-GATA3-FOXP3 pathway that regulates early pathways of Foxp3 expression. These results highlight previously unappreciated links between T_{reg} and Th2 differentiation and extend our understanding of the transcription factors that regulate T_{reg} differentiation and their temporal sequencing. These findings have significant implications for future mechanistic and translational studies of CDK8 and CDK8 inhibitors.

45 **MAIN TEXT**

46 **Introduction**

47 The immune system comprises innate and adaptive immune cells whose collaborative and
48 coordinated responses maintain the healthy state. Each cell type can exert either pro- or anti-
49 inflammatory forces. For example, innate immune cells can secrete either pro- (e.g. IFNγ) or anti-
50 (e.g. IL-10) inflammatory cytokines; similarly, $CD4^+$ T cells can differentiate into either pro- (e.g.
51 Th1, Th17) or anti- (T_{reg}) inflammatory subsets (1-5). These pro- and anti- inflammatory forces
52 must be precisely balanced; dysregulation of this balance can predispose to autoimmunity,
53 infection or cancer (3, 6).

54

55 We have previously demonstrated how small molecules can highlight novel pathways of
56 immunoregulation in primary immune cells. For example, we showed that small molecule
57 inhibition of the dual-specificity tyrosine phosphorylation-regulated kinase 1A (DYRK1A)
58 promotes differentiation of murine and human $CD4^+$ T cells into T_{reg}s (7). We also showed that
59 small molecule inhibition of salt-induced kinases (SIKs) enhanced production of IL-10 by murine
60 and human myeloid cells (8). However, a comprehensive understanding of how both innate and
61 adaptive immune cell function is modulated remains lacking for most small molecules.

62

63 Here, we investigate the effect of the natural product-derived small molecule dihydro-
64 cortistatin A (DCA) on murine and human $CD4^+$ T cells. Recent studies pointing to DCA as the
65 CDK8 inhibitor with highest specificity and lowest toxicity highlight DCA as a CDK8 inhibitor
66 of critical interest (*9*). CDK8 is an essential component of the CDK8 submodule of the Mediator
67 coactivator complex, which regulates RNA polymerase II activity (*10*, *11*). The CDK8 submodule
68 facultatively binds the Mediator complex, phosphorylates transcription factors and regulates
69 specific pathways (*11-13*). CDK8 phosphorylates several immune-relevant transcription factors,

70 including STAT1^{Ser727}, STAT3^{Ser727}, STAT5^{Ser730}, c-Jun^{Ser243} and Notch (*14-19*). CDK8 regulates
71 both innate and adaptive immune responses and CDK8 inhibition typically exerts tolerogenic
72 effects. We previously found that DCA promotes production of IL-10 in myeloid cells by
73 inhibiting cyclin-dependent kinase 8 (CDK8) (*20-22*). Additionally, CDK8 deletion in innate
74 immune NK cells improves tumor surveillance while in adaptive immune cells, CDK8/19
75 inhibitors promote T_{reg} differentiation (*18*, *22-25*). Recent findings that CDK8 inhibition
76 promotes Th17 differentiation suggest the first pro-inflammatory sequelae (*26*). How CDK8
77 regulates differentiation to other T cell lineages (Th1 and Th2) remains less clear. Furthermore,
78 much of the mechanistic work in T cells has focused on CDK8 phosphorylation of STAT5 and
79 STAT3. The possibility of additional CDK8-regulated pathways in the context of T cell biology is
80 suggested by our findings that CDK8 regulates myeloid cells by c-Jun^{Ser243} phosphorylation;
81 however, the identity of these pathways remains incompletely elucidated (*22*). Understanding
82 these pathways is essential to identify the patients who might most benefit from CDK8 inhibition
83 therapy.
84
85 We demonstrate that DCA exerts a unique pattern of immunomodulation (i.e. chemical
86 immunophenotype) compared to other known immunomodulatory small molecules. Using both
87 small molecule inhibitors and CRISPR/Cas9 knockdown, we find that DCA inhibits CDK8 to
88 promote the differentiation of both T_{reg} and Th2 cells while suppressing the differentiation of pro-
89 inflammatory Th1 and Th17 subsets. We show that DCA-driven T_{reg}s are fully suppressive in the
90 absence of concomitant tolerogenic effects on innate immune cells. Mechanistically, CDK8
91 inhibition by DCA regulates T_{reg}/Th17/Th1 differentiation independent of effects on
92 STAT1/STAT3 Ser727 phosphorylation. Notably, DCA's unusual chemical immunophenotype
93 directly leads us to find that DCA uniquely drives early temporal expression of *FOXP3* at least in
94 part via a CDK8-GATA3-FOXP3 pathway not previously described to regulate T_{reg}

95 differentiation. These findings further our mechanistic understanding of an emerging role for
96 DCA as an immunomodulator that broadly drives tolerogenic programs in both innate and
97 adaptive immune cells. These findings are discussed in the context of implications to future
98 therapeutic use of CDK8 inhibitors.

99 **Results**

00

01 **DCA exerts tolerogenic effects on murine and human $CD4^+$ T cell differentiation**

02 Given our previous observation that DCA promotes tolerogenic IL-10 production in innate

03 immune cells, we determined whether DCA exerts tolerogenic effects on $CD4^+$ T cell

04 differentiation (*22*). We tested the effect of DCA on naïve murine $CD4^+$ T cells cultured in

05 suboptimal pro-T_{reg} or -Th2 conditions (T_{reg}^{low} and $Th2^{low}$, respectively) as we previously

06 described (7). DCA enhanced differentiation of both T_{reg} and Th2 cells (Fig. 1A). DCA increased

07 T_{reg}s specifically in cultures of FACS-sorted naïve $CD4^+$ T cells, but not sorted T_{reg}s, further

08 demonstrating that the increase in T_{reg}s is due to enhanced differentiation of T_{reg}s rather than

09 expansion of existing T_{reg}s (Fig. S1A). To examine if these tolerogenic effects extended to

10 inhibiting differentiation of pro-inflammatory T cell lineages, we added DCA to murine T cells

11 cultured in near-optimal pro-Th1 and -Th17 conditions ($Th1^{hi}$ and $Th17^{hi}$, respectively). DCA

12 significantly inhibited differentiation of Th1 and Th17 cells (Fig. 1B). Notably, DCA promoted

13 differentiation of T_{reg} and Th2 cells even in near-optimal $Th17^{hi}$ and $Th1^{hi}$ conditions respectively

14 (Fig. 1B, FACS plots). In the context of non-polarizing Th0 conditions, DCA significantly, albeit

15 modestly, enhanced murine T_{reg} and Th2 differentiation (Fig. 1C). Th1 differentiation was slightly

16 reduced below the level of statistical significance and Th17 cells were too infrequent to accurately

17 assess (Fig. 1C). These results suggest that DCA can enhance T_{reg}/Th2 differentiation in the

18 absence of exogenous cytokines. Therefore, DCA exerts powerful and broad tolerogenic effects

19 on murine T cell differentiation.

20

21 We next investigated whether DCA similarly affects human T_{reg} and Th2 differentiation

22 by culturing human $CD4^+$ T cells in (human-specific) suboptimal T_{reg}^{low} and $Th2^{low}$ conditions

23 respectively. DCA treatment enhanced both T_{reg} and Th2 differentiation in human $CD4^+$ T cells,

24 pointing to concordant regulation in human and murine cells (Fig. 1D-F). We benchmarked the

25 pro-T_{reg} effect of DCA against the well-described T_{reg} enhancers all-trans retinoic acid (ATRA)
26 and rapamycin (RAPA) (*27-33*). In murine and human $CD4^+$ T cells cultured in suboptimal T_{reg}^{low}
27 conditions, DCA treatment enhanced the total number of T_{reg}s significantly higher than either
28 ATRA or rapamycin (Fig. 1D). In addition, DCA enhanced the percentage of T_{reg}s to a level
29 similar to ATRA and rapamycin (Fig. 1E). These results highlight that DCA potently enhances
30 T_{reg} differentiation in both murine and human T cells and reflect in part the lower cytotoxicity of
31 DCA compared to ATRA and rapamycin (Fig. S1B).
32
33 **DCA identifies a novel CDK8 inhibition-driven chemical immunophenotype**
34 We compared DCA's profile of tolerogenic effects against that of other tolerogenic
35 compounds. We investigated the dose-response of murine $CD4^+$ T cells to DCA and two other
36 tolerogenic small molecules in the context of suboptimal pro-T_{reg}, Th2, Th1 and Th17 conditions
37 (T_{reg}^{low}, $Th2^{low}$, $Th1^{low}$ and $Th17^{low}$, respectively) (7). These experiments showed that DCA
38 enhanced differentiation of both murine T_{reg} and Th2 cells with identical EC_{50} (dose exerting half-
39 maximal effect), supporting the involvement of a common mechanistic target (Fig. 2A). We
40 wanted to understand if DCA's ability to enhance T_{reg} and Th2 differentiation and myeloid IL-10
41 production represent a pattern common to many tolerogenic small molecules. We tested harmine,
42 which we previously identified as a potent enhancer of T_{reg} differentiation, and found that
43 harmine enhanced the differentiation of T_{reg}, but not Th2, cells (Fig. 2A) (7). We also tested HG-
44 9-91-01, which we previously showed enhances myeloid cell production of IL-10 production by
45 inhibiting salt-inducible kinase (SIK) 1-3, and found that HG-9-91-01 enhanced neither T_{reg} nor
46 Th2 differentiation (Fig. 2A) (8). Therefore, DCA, HG-9-91-01 and harmine exert distinct
47 immune phenotypic profiles, which we term chemical immunophenotypes, reflecting engagement
48 of distinct pathways regulating tolerogenicity in innate and adaptive immune cells.
49

50 We and others have previously shown immunomodulatory effects of DCA and other
51 CDK8 inhibitors (*18*, *22-25*). We used two different approaches to validate CDK8 as the T_{reg}-
52 relevant mechanistic target of DCA. Firstly, we tested DCA alongside a structurally distinct small
53 molecule CDK8 inhibitor, BRD-6989 (*22*). In T_{reg}^{low} conditions, both CDK8 inhibitors showed
54 concentration-dependent enhancement of murine T_{reg} differentiation with EC_{50} for each
55 compound similar to that observed for enhancing IL-10 production in BMDCs (Fig. 2B) (*22*). The
56 EC_{50} of DCA was much lower than of BRD-6989, driving its subsequent preferential use (Fig.
57 2B). Notably, DCA and BRD-6989 both exhibited low cytotoxicity, even less than that observed
58 with harmine, which we previously identified as one of the least cytotoxic T_{reg} enhancers (Fig.
59 2B) (7). Secondly, we used CRISPR/Cas9 to knock out *CDK8* in primary human $CD4^+$ T cells.
60 Efficient editing of CDK8 led to enhanced T_{reg} differentiation comparable to levels observed
61 using DCA treatment (Fig. 1E and 2C). These results indicate that DCA enhances murine and
62 human T_{reg} differentiation at least in part by inhibiting CDK8.
63
64 **DCA-driven T_{reg}s are fully tolerogenic in the absence of DCA-innate immune tolerogenic**
65 **effects**
66 We next interrogated the suppressive capacity of DCA-driven T_{reg} cells both in vitro and
67 in vivo. Using a standard in vitro suppression assay, we observed no significant differences in the
68 ability of T_{reg}^{hi}- or $T_{reg}^{low+DCA}$-driven murine T_{reg} cells to suppress proliferation of co-cultured
69 responder $CD4^+$ T cells (Fig. 3A, red and blue lines respectively). We tested the capacity of DCA-
70 driven T_{reg}s to inhibit inflammation in vivo in two murine T_{reg}-transfer models in order to exclude
71 confounding effects of systemically-delivered DCA on endogenous innate immune cells. In an
72 established model of type 1 diabetes, transfer of NOD-*BDC2.5*$^+$ $CD4^+$ T cells, specific for an
73 epitope derived from the islet antigen chromogranin A, into NOD-*scid* recipients results in islet β-
74 cell destruction and onset of diabetes about 10 days later (Fig. 3B, black line) (*34*, *35*). Co-

injection of antigen-specific T_{reg} cells, generated from naïve NOD-*BDC2.5.Foxp3*$^{IRES\text{-}GFP}$ CD4$^+$ T cells using either $T_{reg}^{low+DCA}$ or T_{reg}^{hi} conditions, significantly delayed onset of diabetes to a similar degree (Fig. 3B, blue and red lines respectively) (7). We observed similar results in a murine model of intestinal inflammation where transfer of CD45RB^{hi}CD4$^+$ T cells into B10.RAG2$^{-/-}$ recipients results in expansion of donor T cells and inflammation most prominent in the colon about 4 weeks later (Fig. 3C, black) (*36*, *37*). Co-transfer of T_{reg} cells, generated from naïve wild-type C57Bl/6 CD4$^+$ T cells using either $T_{reg}^{low+DCA}$ or T_{reg}^{hi} conditions, resulted in significant and similar attenuation of intestinal inflammation (Fig. 3C, blue and red respectively) (*38*). Together, these results demonstrate that DCA-driven T_{reg} cells are fully functional and equivalent to T_{reg}^{hi}-generated T_{reg} cells (an adoptive cellular therapy-relevant gold standard comparison) both in vitro and in vivo, using model systems employing different genetic backgrounds and T cell specificities. Importantly, these experiments demonstrate that DCA exerts a strong T_{reg}-intrinsic tolerogenic effect in the absence of concomitant effects on the innate immune compartment.

DCA exerts tolerogenic effects on T cell differentiation independent of regulating STAT1^{Ser727}, STAT3^{Ser727} and c-Jun^{Ser243} phosphorylation

We investigated key candidates that might account for DCA's tolerogenic effects in CD4$^+$ T cells. CDK8 phosphorylates STAT1^{Ser727} and STAT3^{Ser727} in several cell types (*39-42*). Although the role of Ser727 phosphorylation in Th1/Th17/T_{reg} differentiation is unclear, potential contribution is suggested by the central role of STAT1^{Tyr701} and STAT3^{Tyr705} tyrosine phosphorylation in Th1 and Th17 differentiation respectively (*43-45*). Recent studies argue that inhibition of CDK8 promotes Th17 differentiation by attenuating STAT3^{Ser727} phosphorylation, emphasizing the importance of investigating this pathway (*26*). DCA reduced IL-6-induced STAT3^{Ser727} phosphorylation in murine CD4$^+$ T cells, but did not reduce either STAT3^{Tyr705}

00 phosphorylation or expression of the hallmark Th17 transcription factor RORγt in cells cultured
01 in Th17^{hi} conditions; total STAT3 was slightly decreased (Fig. 4A-C). Primary CD4^{+} T cells from
02 *Stat3^{Ser727Ala}* mice, in which Ser727Ala mutation abrogates STAT3^{Ser727} phosphorylation, showed
03 reduced Th17 differentiation, highlighting a previously unappreciated role of STAT3^{Ser727}
04 phosphorylation in this process (Fig. 4D) (*40*). However, DCA suppressed Th17 and enhanced
05 T_{reg} differentiation in both *Stat3^{Ser727Ala}* and wild-type CD4^{+} T cells, demonstrating that DCA
06 regulates T_{reg} and Th17 differentiation via mechanisms independent of STAT3^{Ser727}
07 phosphorylation (Fig. 4D-E).
08
09 We also showed that DCA reduced IFNγ-induced phospho-STAT1^{Ser727} but not of
10 phospho-STAT1^{Tyr701} or total STAT1 in cells cultured in Th1^{hi} conditions (Fig. 4F-G). Expression
11 of the hallmark Th1 transcription factor Tbet in Th1^{hi} cultures was also unaltered by DCA except
12 at day 4, arguing against altered regulation by STAT1^{Ser727} (Fig. 4H). Primary CD4^{+} T cells from
13 *Stat1^{Ser727Ala}* mice, in which Ser727Ala mutation abrogates STAT1^{Ser727} phosphorylation, showed
14 reduced Th1 differentiation, highlighting a previously unappreciated role of STAT1^{Ser727}
15 phosphorylation in this process (Fig. 4I) (*41*). However, DCA suppressed Th1 and enhanced T_{reg}
16 differentiation in both *Stat1^{Ser727Ala}* and wild-type CD4^{+} T cells, demonstrating that DCA regulates
17 T_{reg} and Th1 differentiation via mechanisms independent of STAT1^{Ser727} phosphorylation (Fig. 4I-
18 J).
19
20 Consistent with previously published findings, we also found that treatment with DCA
21 inhibited IL-2-induced phosphorylation of STAT5b^{Ser730} (Fig. S2A) (*18*). We were unable to find
22 *Stat5b^{Ser730Ala}* mice to perform similar studies as with STAT1 and STAT3 above.
23

24 We next investigated the overlap between characterized CDK8-regulated pathways in
25 innate and adaptive immune cells. Similar to our findings in myeloid cells, T cells cultured in
26 either T_{reg}^{low} or T_{reg}^{hi} conditions showed increased phosphorylation of both c-Jun^{Ser243} and c-
27 Jun^{Ser63}; DCA specifically inhibited phosphorylation on the inhibitory site c-Jun^{Ser243} (Fig. S2B)
28 (*22*). Unlike in myeloid cells, DCA's tolerogenic pro-T_{reg} effect in T cells was neither attenuated
29 by the AP-1 inhibitor T-5224 nor enhanced by overexpression of multiple c-Jun family members
30 (c-Jun, JunB or JunD) (Fig. S2C-D). Together, these results indicate that DCA regulation of AP-1
31 transcription factors drives tolerogenicity in myeloid, but not $CD4^+$ T, cells.
32
33 **DCA enhances Foxp3 expression by engaging GATA3**
34 Temporal flow cytometric analysis of FOXP3 expression throughout the period of culture
35 revealed indistinguishable kinetics between murine $CD4^+$ T cells cultured in T_{reg}^{low} and T_{reg}^{hi}
36 conditions until day 2, with $FOXP3^+$ cells increasing in T_{reg}^{hi} conditions and decreasing in T_{reg}^{low}
37 conditions thereafter (Fig. 5A) (7). Notably, DCA treatment significantly increased $FOXP3^+$ cells,
38 as well as *Foxp3* expression, at early time points (days 1 and 2) compared to either T_{reg}^{low} or T_{reg}^{hi}
39 conditions (Fig. 5A-B). DCA treatment also drove concordant regulation of other FOXP3-
40 regulated genes at day 2, including upregulation of *Eos, Helios* and *Cd25* as well as
41 downregulation of *Il2* expression (Fig. 5B) (*46-49*). These data suggest that DCA promotes
42 murine T_{reg} differentiation at least in part by enhancing early expression of FOXP3. This
43 induction of key T_{reg} transcription factors did not involve canonical T_{reg} pathways; specifically,
44 DCA neither enhanced SMAD2/SMAD3 nor inhibited (mTOR pathway members) S6/S6K
45 phosphorylation, pointing to the involvement of novel pathway(s) (Fig. S3A-B).
46
47 DCA's unusual chemical immunophenotype led us to consider a mechanistic link between
48 DCA-mediated enhancement of both T_{reg} and Th2 differentiation. GATA3, the hallmark Th2

49 transcription factor, is highly expressed beginning at the earliest timepoints of Th2 differentiation
50 (*50*). Although not well studied in the context of T_{reg} differentiation, previous findings that
51 GATA3 binds the CNS2 enhancer element of the *FOXP3* locus and regulates mature T_{reg}
52 physiology support the possibility that GATA3 could regulate FOXP3 expression and thus T_{reg}
53 differentiation (*51-53*). Consistent with this notion, DCA treatment of both murine and human
54 $CD4^+$ T cells cultured in T_{reg}^{low} conditions also enhanced early *GATA3* expression at day 2 (Fig.
55 5C). To validate the role of DCA-mediated upregulation of GATA3 in T_{reg} differentiation, we
56 generated lentiviral vectors to overexpress *GATA3*, including a truncated NGFR marker separated
57 by a self-splicing T2A peptide to allow specific comparison of transduced cells. We performed
58 these experiments using human T cells because these were more amenable to viral transduction.
59 Overexpression of *GATA3* consistently enhanced T_{reg} differentiation in human naïve $CD4^+$ T cells
60 cultured in T_{reg}^{low} conditions, compared to cells transduced with control (NGFR only) virus (Fig.
61 5D). To further support the functional significance of DCA-enhanced GATA3, we performed
62 chromatin immunoprecipitation experiments and found that DCA treatment of human $CD4^+$ T
63 cells cultured in T_{reg}^{low} conditions resulted in significantly increased binding of GATA3
64 specifically to *FOXP3* CNS2 early in T_{reg} differentiation (Fig. 5E). These results argue that
65 GATA3 is an early regulator of *FOXP3* expression and T_{reg} differentiation that can be regulated
66 by DCA.
67
68 We sought to better understand how DCA might regulate *GATA3* expression. Previous
69 studies showed that Notch can directly drive *Gata3* expression and that enhanced Notch signaling
70 promotes T_{reg} differentiation (*54*, *55*). Furthermore, CDK8 inhibits Notch signaling by
71 phosphorylating the Notch signaling domain ICD1, leading to its degradation, leading us to
72 hypothesize that DCA may drive *Gata3* expression by enhancing Notch signaling in T cells (*19*).
73 Consistent with this notion, we found that treatment with DCA led to increased intranuclear levels

74 of ICD1 in both murine and human $CD4^+$ T cells (Fig. 5F). Supporting functional relevance of
75 DCA-driven increased intracellular ICD1, we performed RNAseq analyses comparing $FOXP3^+$
76 cells cultured for 2 days in T_{reg}^{low} versus $T_{reg}^{low+DCA}$ conditions to define a 577-gene signature
77 associated with DCA treatment. Using a previously described method, we showed that this
78 signature is maintained in sorted mature $FOXP3^+$ iT_{reg}s generated after 4 days of culture in
79 $T_{reg}^{low+DCA}$ versus T_{reg}^{hi} conditions and partially maintained in $FOXP3^+$ versus $FOXP3^-$ cells
80 cultured for 2 days in T_{reg}^{low} conditions, supporting FOXP3- and T_{reg}-relevance of this signature
81 (Fig S4) (*7*, *56*). Transcription factor target analysis of this DCA signature using the ChIP-seq
82 result-based Gene Transcription Regulation Database (GTRD) in GSEA revealed MAML as the
83 most enriched transcription factor (Table S1) (*57-59*). MAML is recruited by DNA-bound ICD1,
84 in complex with RBP-J, whereupon it recruits transcriptional co-activators (*60*). Therefore,
85 enrichment of MAML binding sites is consistent with enrichment of ICD1 binding to DCA-
86 regulated genes. Together, these results demonstrate for the first time that inhibition of CDK8 by
87 DCA drives *FOXP3* expression and T_{reg} differentiation at least in part by driving increased Notch
88 and GATA3 signaling.
89

90 **Discussion**

91 Here we have demonstrated that DCA promotes T_{reg} differentiation at least in part by
92 engaging a previously unappreciated CDK8-GATA3-FOXP3 pathway. Our use of both novel
93 small molecules (DCA and BRD-6989) and CRISPR/Cas9-mediated deletion point to CDK8
94 inhibition as the mechanism by which DCA exerts these effects. While previous studies have
95 shown that GATA3 impacts mature T_{reg} physiology, this is the first report to our knowledge that
96 GATA3 can drive T_{reg} differentiation (*51*, *61*). Our findings extend prior studies showing that
97 GATA3 protein levels are upregulated during T_{reg} differentiation (*62*). Whether GATA3 initiates,
98 stabilizes or amplifies *FOXP3* expression remains to be dissected in future studies. Previous
99 reports suggesting that GATA3 inhibits FOXP3 expression used significantly different
100 experimental approaches, including secondary CD3 stimulation or removal of primary TCR
101 stimulation, and did not exclude contribution of IL-4 (*63*, *64*). Given that GATA3 is a hallmark
102 Th2 transcription factor that inhibits Th1 and likely Th17 differentiation, this CDK8-GATA3-
103 FOXP3 pathway provides a parsimonious unifying mechanism to explain, at least in part, how
104 DCA broadly regulates T_{reg}, Th2, Th1 and Th17 differentiation (*65-67*). Given that Th2 cells can
105 produce IL-10, this previously unappreciated link between T_{reg} and Th2 differentiation may point
106 to conserved (e.g. CDK8-related) anti-inflammatory signaling pathways that can engage distinct
107 downstream effector pathways (*68*). We hypothesize that differences in the local cytokine milieu
108 impact whether DCA enhances T_{reg} or Th2 differentiation, for example by modulating epigenetic
109 accessibility of *FOXP3* and *IL4* loci. Additionally, where CDK8 effector pathways regulating
110 tolerogenicity in innate (via phospho-c-Jun^{Ser243}) vs adaptive immune cells diverge remains to be
111 clearly defined (*22*).
112
113 Our discovery of DCA's unusual temporal profile of enhancing early expression FOXP3
114 and many FOXP3-regulated genes contrasts with the temporal profile of T_{reg}^{hi} conditions and

15 other T_{reg}-enhancing compounds like harmine and reinforces a model of T_{reg} differentiation that
16 involves independently regulated early and late pathways (7). Whereas early pathways might
17 involve TGFβ licensing cells to adopt T_{reg} fate and express FOXP3, late pathways might maintain
18 and promote T_{reg} lineage commitment. Our data support a model where DCA largely enhances
19 early pathways, including Notch-GATA3, to regulate FOXP3 expression. This suggests DCA
20 may have particular therapeutic relevance to patients who have defects in early pathways of T_{reg}
21 differentiation and also raises the possibility of synergy with therapies that enhance late pathways
22 of T_{reg} differentiation.
23
24 Our findings exemplify how chemical immunotypes point to an important classification
25 scheme that can inform both mechanistic and therapeutic hypotheses. DCA's unique chemical
26 immunophenotype (pro-T_{reg}, pro-Th2 and pro-myeloid-IL-10) is distinct from that of many other
27 tolerogenic compounds, including SIK- and DYRK1A-inhibitors, which exert tolerogenic effects
28 specifically in either innate or adaptive immune cells, but not both (*7*, *22*). Our novel finding that
29 CDK8 inhibition promotes both T_{reg} and Th2 differentiation directly informed our interrogation of
30 GATA3 as a putative regulator of T_{reg} differentiation. Additionally, our studies suggest value in
31 monitoring tolerogenic effects, including impaired host-versus-tumor effects, in anticipated
32 clinical use of CDK8 inhibitors as cancer therapeutics (*69*, *70*).
33
34 The translational relevance of these data is reinforced by our finding that DCA promotes
35 T_{reg} differentiation in primary human $CD4^+$ T cells. We note that T_{reg}s generated using DCA are
36 fully functional in vitro and in vivo. Importantly, our use of T_{reg}-transfer models specifically
37 interrogates the functionality of DCA-driven T_{reg}s without confounding anti-inflammatory effects
38 on innate immune cells, that could confound the interpretation of models using systemic drug
39 administration (*18*, *25*). DCA and other CDK8 inhibitors may find utility as tolerogenic

40 immunomodulators. Studies suggesting poor long-term tolerability of CDK8 inhibitors, together
41 with our data showing DCA impacts early pathways in T_{reg} differentiation, support this
42 consideration (*71*). We recognize the utility of DCA in generating T_{reg}s ex vivo, which would
43 circumvent concerns regarding toxicity in vivo (*71*).
44
45 Our findings highlight the value of definitive interrogation of regulatory pathways. Prior
46 knowledge drove the notion of CDK8-STAT interactions as key candidates to explain how CDK8
47 inhibition regulates T cell differentiation (*14*). Our experiments using *Stat1*^{Ser727Ala} and
48 *Stat3*^{Ser727Ala} mice clearly demonstrate that DCA regulates Th1, Th17 and T_{reg} differentiation
49 independent of its effects on STAT1^{Ser727}/STAT3^{Ser727} phosphorylation. Prior studies suggest that
50 STAT1^{Ser727}/STAT3^{Ser727} phosphorylation is required for full transcriptional activity (*39-42*).
51 Consistent with this, we demonstrate a previously unappreciated role of STAT1^{Ser727} and
52 STAT3^{Ser727} phosphorylation in positively regulating Th1 and Th17 differentiation respectively.
53 These findings differ from recent studies suggesting that CDK8 inhibition promotes human Th17
54 differentiation; possible explanations include differences in species, CDK8 inhibitor and
55 experimental approach (knockin versus transduced allele) (*26*). This emphasizes the value of Ser-
56 Ala STAT mutant mice in dissecting (CDK8-related) mechanistic hypotheses, including
57 developing *Stat5b*^{Ser730Ala} mice to definitively define the role of CDK8-regulated STAT5b^{Ser730}
58 phosphorylation in T_{reg} differentiation (*18*). These findings have important implications for
59 disease pathobiology and precision therapy, for example suggesting synergy of therapeutically
60 targeting STAT1^{Tyr701}/STAT3^{Tyr705}, STAT1^{Ser727}/STAT3^{Ser727} and CDK8.
61
62 In summary, our studies highlight CDK8 as a regulator of innate and adaptive immune
63 tolerogenicity that is therapeutically targeted by the high-specificity low-toxicity inhibitor DCA
64 (*9*). We show for the first time that CDK8 regulates Th2 differentiation, and human T_{reg}

65 differentiation. The unique chemical immunophenotype of DCA (pro-T_{reg}/Th2) directly informs
66 the discovery of a novel CDK8-Notch-GATA3-FOXP3 axis that regulates early pathways of T_{reg}
67 differentiation and has further mechanistic and therapeutic implications. Our demonstration that
68 DCA effectively enhances T_{reg} differentiation compared to canonical T_{reg} enhancers suggests
69 utility in approaches to generate T_{reg}s ex vivo for adoptive cellular therapy. In addition, the
70 broadly tolerogenic effects of DCA suggest that it may broadly be useful in the setting of
71 pathologic inflammation or autoimmunity.

72 **Materials and Methods**

73 **Mice**

74 Balb/c RRID:IMSR_JAX:000651, C57Bl/6 000664RRID:IMSR_JAX:000664, *Foxp3*$^{IRES\text{-}GFP}$

75 RRID:IMSR_JAX:006772*, CD45.1*$^{+/+}$002014RRID:IMSR_JAX:002014*,* NOD-*scid* and NOD-

76 *BDC2.5* mice were purchased from Jackson Labs. NOD-*BDC2.5.Foxp3*$^{IRES\text{-}GFP}$ mice were from

77 the JDRF Transgenic Core (Harvard Medical School, Boston, MA). C57Bl/10-*Rag2*$^{-/-}$ mice were

78 a kind gift from Brian Kelsall (*37*). *Stat1*^{Ser727Ala} and *Stat3*^{Ser727Ala} mice were previously described

79 (*40*, *41*). Mice were housed in the Benaroya Research Institute Vivarium in a SPF animal room

80 with unfettered access to food and water. All murine experiments were performed on male and

81 female mice between 7-12 weeks of age, with the approval of the IACUC of Benaroya Research

82 Institute (Seattle, WA).

83

84 **Human samples**

85 Frozen PBMCs and fresh peripheral blood samples were obtained from the Benaroya Research

86 Institute Immune Mediated Disease Registry and Repository. Human studies were approved by

87 the Benaroya Research Institute's Institutional Review Board and all subjects signed written

88 informed consent prior to inclusion in the study.

89

90 **Cell lines**

91 293T cells used in lentiviral production were a generous gift from David Rawlings. 293T cells are

92 female. They were cultured DMEM medium (Hyclone) supplemented with fetal bovine serum

93 and glutamax (Thermo fisher) at 37°C and 5% CO2. Cells were split every 3 days at a density of

94 7.5x10^4 cells per ml.

95

96 **Small Molecules and Reagents**

97 Δ16-cortistatin A (DCA) was a generous gift from P. Baran (The Scripps Research Institute) and
98 synthesized as previously reported (*20*, *72*). Small-molecule reagents were confirmed to have
99 ≥95% purity by HPLC–MS. Antibodies, chemical reagents and cytokines were sourced as listed
00 in Table S2. Primers are listed in Table S3
01

02 **Cloning and Plasmid Preparation**

03 Coding sequences of GATA3, JUND, c-JUN and JUNB were PCR amplified from pHAGE-
04 GATA3, JunD-HA neo, pMIEG3-c-Jun and pMIEG3-JunB (Addgene #116747, 58515, 40348
05 and 40349, gifts from Gordon Mills & Kenneth Scott, Kevin Janes, and Alexander Dent
06 respectively). PCR overhang extension was used to add (i) self-splicing T2A sequence and (ii) 40
07 base pair homology arms (HA) to permit cloning into into EcoRV-digested pLKO.NGFR using
08 Gibson assembly ultra-kit (Codex DNA, San Diego, CA). Primers used are listed in Table S2.
09

10 **Murine T cell isolation and culture**

11 Unless otherwise noted, $CD4^+$ $CD62L^+$ naïve T cells were isolated from 8-12 week-old mice
12 using CD4 negative enrichment kits (Stemcell Technologies, Vancouver, Canada) and CD62L
13 microbeads (Miltenyi Biotec, San Diego, CA) according to the manufacturer's instructions and
14 confirmed >90% pure by flow cytometry. Cells were cultured on 96 well plates pre-coated with
15 anti-CD3 and anti-CD28 using conditions outlined in Table S4. The addition of DCA to T_{reg}^{low}
16 conditions is abbreviated as $T_{reg}^{low+DCA}$. T_{reg} and Th1 cultures were fed with equal volume of IL-2
17 supplemented media (20ng/ml) and retreated with compound at day 2, split 1:2 into IL-2-
18 supplemented media (10 ng/ml) at day 3 and analyzed at day 4. Th17 cultures were treated
19 similarly except no IL-2 was supplemented. Th2 cultures were treated similarly as T_{reg} cultures
20 except they were additionally split 1:2 into IL-2 supplemented media (10 ng/ml) at day 4 and day
21 5 and analyzed on day 6. To assess STAT1/STAT3/STAT5b Ser phosphorylation, cells were

22 stimulated with 10 ng/ml IFNγ + 2μg/ml anti-IL-4, 10 ng/ml IL-6 + 2 μg/ml each anti-IL4/-12/-
23 IFNγ and anti-CD3/CD28 + 100 ng/ml IL-2 respectively.
24
25 **Human T cell isolation and culture**
26 Frozen PBMCs and fresh peripheral blood samples were obtained from the Benaroya Research
27 Institute Immune Mediated Disease Registry and Repository. Human peripheral blood
28 mononuclear cells were isolated from fresh whole blood by Ficoll-Paque (GE Healthcare, Little
29 Chalfont, United Kingdom). $CD4^+CD45RA^+$ naïve T cells were isolated using negative
30 enrichment kits (Stemcell Technologies, Vancouver, Canada) per manufacturer's instructions and
31 confirmed >90% pure by flow cytometry. Cells were cultured on 96 well plates pre-coated with
32 anti-CD3 and anti-CD28 using conditions outlined in Table S4. T_{reg} cultures were fed with equal
33 volume of IL-2 supplemented media (20ng/ml) and retreated with compound at day 2, split 1:2
34 into IL-2-supplemented media (10 ng/ml) at day 4 and analyzed at day 5. Th2 cultures were fed
35 and split into media supplemented with IL-2+IL-4 (20 ng/ml each at day 2, 10 ng/ml each
36 thereafter) and compound as indicated to maintain ~10^6 cells/ml, restimulated on days 7 and 14
37 on plates pre-coated with anti-CD3 and anti-CD28 and analyzed at day 21 as previously described
38 (*73*).
39
40 **Lentiviral Production**
41 On day 0, 3.8 x 10^6 293T cells were plated in 10 ml DMEM + 5% Glutamax (Thermofisher) on a
42 10 cm plate. On day 1, cells were transfected with 1.5 μg pMD2G, 3 μg psPAX2 (kind gifts from
43 David Rawlings) and 6 μg of pLKO vector, mixed with 42 μg PEI transfection reagent
44 (Polysciences, Inc.) and suspended in 0.5 ml diluent (10 mM HEPES, 150mM NaCl, pH 7.05).
45 Cells were PBS-washed and fed with fresh DMEM + Glutamax on day 2. Viral supernatant was
46 harvested on day 4, centrifuged (2000 rpm x 5 mins) to remove cellular debris, overlaid onto 5 ml

47 of 10% sucrose in NTE (135 mM NaCl, 10mM TrisCl, ph 7.50, 1mM EDTA) in ultra-centrifuge
48 tubes (Beckman) and centrifuged at 25,000 rpm for 90 minutes at 4°C. Supernatant was removed
49 and viral pellet resuspended in ice cold NTE by shaking for 2 hours at 4°C.
50
51 **RNP complexing**
52 RNPs were generated by mixing 1.25 ug Cas9 protein (Aldevron, Fargo, ND) and 2.5 pmol each
53 of 3 sgRNAs (Synthego, Menlo Park, CA) with gentle swirling, and incubating at 37°C for 15
54 minutes. Guides used were CDK8: CUCAUGCUGAUAGGAAG,
55 UGUUUCUGUCUCAUGCUGAU, and UCUGUCUCAUGCUGAUAGGA.
56
57 **CRISPR-Cas9 gene editing**
58 CRISPR-Cas9 gene editing was performed as previously described with modifications (Aksoy et
59 al., 2020; Roth et al., 2018). Briefly, human $CD4^+CD45RA^+$ naïve T cells were cultured on 96
60 well plates pre-coated with anti-CD3 and anti-CD28 in TCM supplemented with 5% Fetal Bovine
61 Serum, 20 ng/ml IL-2 and 2 μg/ml each of anti-IL-12, anti-IFNγ and anti-Il-4. Cells were
62 harvested 2 days later, centrifuged (90 g for 8 minutes), resuspended in buffer T, mixed with
63 20μM of each RNP complex and electroporated (1600 volts, 10 ms, 3 pulses) using a Neon
64 transfection system (Thermo Fisher, Waltham, MA). Cells were transferred into 90 μl TCM pre-
65 warmed to 37°C. After 24 hours, cells were fed with media supplemented with 100 ng/ml IL-2
66 and 1 ng/ml TGFβ. Cells were maintained for 5 additional days at a density of $1x10^6$/ml and then
67 analyzed by flow cytometry.
68
69 **Flow Cytometry**
70 Cells were stimulated with PMA and ionomycin (50 and 500ng/ml respectively) (Sigma Aldrich,
71 St. Louis, MO) in the presence of Golgistop (BD Biosciences, San Jose, CA) 5 hours prior to

72 analysis as necessary. Cells were typically stained with LIVE/DEAD (Thermo Fisher, Waltham,
73 MA) and anti-CD4 prior to fixation and permeabilization, which was generally performed with
74 either Foxp3 fixation/permeabilization buffers (eBioscience, San Diego, CA). Phosflow cell
75 lyse/fix and PermIII buffers (BD Biosciences, San Jose, CA) were used for phospho-protein
76 assessment. Intracellular staining was performed per manufacturer's instructions. Counting beads
77 (10 μm, Spherotech, Lake Forest, IL) were added at 5000 per sample. Acquisition was performed
78 on either a FACScalibur or a FACScanto (BD Biosciences, San Jose, CA). Cell sorting was
79 performed using a FACs Aria II (BD Biosciences, San Jose, CA). Data was analyzed using
80 FlowJo software (Treestar, Ashland, OR). Fractional maximal enhancement was determined by
81 increase in percentage lineage-committed cells, relative to maximal cytokine-driven enhancement
82 as previously reported (7). Fractional inhibition was calculated relative to DMSO treated cells (7).
83 STAT1/STAT3 phosphorylation was quantified as previously described (*74*).
84

85 **In vitro proliferation and T_{reg} suppression assay**

86 These were performed as previously described (*75*). Briefly, sorted $CD45.1^{+}CD4^{+}CD62L^{+}$
87 $T_{responders}$ were labeled with CellTrace Far Red (Thermo Fisher, Waltham, MA) per manufacturer's
88 protocol and plated at $5x10^{4}$ cells per well in 96-well U-bottom plates in the presence of anti-CD3
89 anti-CD28 beads (Dynabead, Grand Island, NY). For T_{reg} suppression assays, $T_{responders}$ were co-
90 cultured with sorted $CD45.2^{+}Foxp3^{IRES\text{-}GFP+}$ T_{reg} cells generated as indicated. Cells were analyzed
91 by flow cytometry 3 days later.
92

93 **T_{reg} suppression – Type 1 diabetes model**

94 These were performed as previously described (7). Briefly, $5x10^{4}$ sorted $CD4^{+}CD62L^{+}$ naïve T
95 cells isolated from NOD-*BDC2.5*$^{+}$ mice were injected intravenously into NOD-*scid* mice with or
96 without $1x10^{5}$ T_{reg} cells generated from NOD-*BDC2.5*$^{+}$*FOXP3*$^{IRES\text{-}GFP}$ mice as indicated (*34*, *35*).

97 Blood glucose levels were monitored with a handheld Contour glucometer (Bayer, Leverkusen,
98 Germany) at days 3, 6, 8 and every day following. Diabetes was diagnosed when blood sugar
99 exceeded 250 mg/dl for 2 consecutive days.
00

01 **T_{reg} suppression – CD45RB^{hi} colitis model**

02 As previously described 5x10^5 sorted CD4$^+$CD62L$^+$ naïve T cells isolated from CD45.1$^+$ mice
03 were injected intravenously into B10-*Rag2*$^{-/-}$ mice (*37*, *38*). 5 days later, mice were injected with
04 either PBS or 1.5x10^5 T_{reg} cells generated from Foxp3$^{IRES-GFP}$ mice as indicated (*38*). Mice were
05 monitored at least weekly for weight loss and morbidity per protocol. Mice were euthanized after
06 4 weeks and proximal, medial, and distal colon analyzed histologically by blinded observers as
07 previously described (*76*).
08

09 **Histology**

10 Tissues were preserved in 10% formalin. Paraffin embedding, sectioning and staining with
11 hematoxylin and eosin was performed by the Histology Core (Benaroya Research Institute,
12 Seattle, WA).
13

14 **Western Blotting**

15 Cells were washed in PBS and lysed in either TNN lysis buffer, pH 8 (100 mM TRIS-HCl, 100
16 mM NaCl, 1% NP-40, 1 mM DTT, 10 mM NaF) or RIPA lysis buffer (150 mM NaCl, 1% Triton
17 X-100, 0.5% sodium deoxycholate, 0.1% SDS, 50 mM TRIS-HCl at pH7.8) supplemented with
18 DTT, protease inhibitors (Roche, Indianapolis, IN) and phosphatase inhibitors (Cell Signaling
19 Technologies, Danvers, MA). Lysates were separated by SDS-PAGE using Tris-Glycine gels
20 loaded with about 1x10^6 cell equivalents per well and transferred onto PDVF membrane
21 (Millipore, Burlington, MA). Blots were blocked in either 5% Milk (Nestle, Vervey, Switzerland)

22 or bovine serum albumin (Sigma Aldrich, St. Louis, MO) and visualized with Western Lightning
23 Plus-ECL (Perkin Elmer, Waltham, MA) and/or SuperSignal West Femto substrate (Thermo
24 Scientific, Waltham, MA) per manufacturer's instructions. Nuclear isolation was performed using
25 Nuclei EZ Prep kit per manufacturer's instructions (Sigma Aldrich, St. Louis, MO). Fractions
26 were subsequently lysed with Triton X-100 lysis buffer (1% Triton X-100, 150 mM NaCl, 50 mM
27 Tris-HCl pH7.8). Band intensity was quantified by ImageJ (*77*).
28

29 **RNA Isolation and qRT-PCR**

30 RNA was isolated using RNeasy kits (Qiagen, Valencia, CA) and cDNA generated using iScript
31 cDNA synthesis kits (BioRad, Hercules, CA) per manufacturer's directions. Real-time PCR was
32 performed using an ABI 7500 FAST REAL-TIME PCR (Applied Biosystems, Foster City, CA)
33 system. Cycling conditions were as follows; 1 cycle of 50°C for 2 minutes, 95°C for 10 minutes,
34 followed by 40 cycles of 95°C for 15 seconds, and 60°C for 1 minute. Primers used are listed in
35 Table S3.
36

37 **RNA-seq library preparation and sequencing**

38 RNA-seq libraries were generated from four *Foxp3*^{GFP} littermate mice. On day 0, 1000 naïve
39 CD4^{+}CD62L^{+} cells were sorted for RNA-seq. The remaining cells were cultured on plates pre-
40 coated with anti-CD3 and anti-CD28 in T_{reg}^{low}, T_{reg}^{hi} and $T_{reg}^{low+DCA}$ conditions. On day 2, 250
41 FOXP3^{+} cells and 500 FOXP3^{-} cells were sorted from cells cultured in T_{reg}^{low}, T_{reg}^{hi} and
42 $T_{reg}^{low+DCA}$ conditions. On day 4, 1000 FOXP3^{+} cells were sorted from T_{reg}^{hi} and $T_{reg}^{low+DCA}$
43 cultures. Cells were sorted directly into lysis buffer from the SMART-Seq v4 Ultra Low Input
44 RNA Kit for Sequencing (Takara) and frozen until all samples were ready for simultaneous
45 processing. Reverse transcription was performed followed by PCR amplification to generate full
46 length amplified cDNA. Sequencing libraries were constructed using the NexteraXT DNA sample

47 preparation kit (Illumina) to generate Illumina-compatible barcoded libraries. Libraries were
48 pooled and quantified using a Qubit® Fluorometer (Life Technologies). Dual-index, single-read
49 sequencing of pooled libraries was carried out on a HiSeq2500 sequencer (Illumina) with 58-base
50 reads, using HiSeq v4 Cluster and SBS kits (Illumina) with a target depth of 5 million reads per
51 sample.
52
53 Base-calling was performed automatically by Illumina real time analysis software.
54 Demultiplexing to generate FASTQ files was performed by bcl2fastq running on the Illumina
55 BaseSpace platform. Subsequent processing was performed using the Galaxy platform. FASTQ
56 reads were trimmed in two steps: 1) hard-trimming to remove 1 3'-end base (FASTQ Trimmer
57 tool, v.1.0.0); 2) quality trimming from both ends until minimum base quality for each read ≥ 30
58 (FastqMcf, v.1.1.2). Reads were aligned to the GRCm38 mouse reference genome using STAR
59 v.2.4.2a, with gene annotations from GRCm38 Ensembl release number 91 (*78*). Read counts per
60 Ensembl gene ID were quantified using htseq-count v.0.4.1 (*79*). Sequencing, alignment, and
61 quantitation metrics were obtained for FASTQ, BAM/SAM, and count files in Galaxy using
62 FastQC v0.11.3, Picard v1.128, Samtools v1.2, and htseq-count v.0.4.1 (*80*). RNAseq data were
63 then processed using Tidyverse, Biomart, EdgeR and limma to generate relative expression values
64 (*81-84*). The raw RNA-seq data has been deposited to the Gene Expression Omnibus (GEO) with
65 accession number GSE141933.
66
67 **Pathway Analysis**
68 Pathway analysis was performed using the Gene Set Enrichment Analysis Molecular Signature
69 Database or MSigDB v7.0 which uses the hypergeometric distribution on a background of all
70 genes to calculate a p-value (*58*, *85*, *86*).
71

72 **Microscale Chromatin Immunoprecipitation Assay**

73 Assay was performed as described previously with few modifications (*87*). 100,000 naïve $CD4^+$
74 T-cells were cultured in T_{reg}^{low} and $T_{reg}^{low+DCA}$ conditions for 2 days and then harvested, washed
75 with ice cold PBS, fixed using 10% v/v of 11% formaldehyde (diluted from 36% stock in 50mM
76 HEPES pH 7.5, 100 mm NaCl, 1 mM EDTA, 0.5 mM EGTA) for 10 minutes, quenched using 5%
77 v/v 2.5 M glycine for 5 minutes, washed twice with 1ml ice-cold PBS and lysed in 50 µl lysis
78 buffer (50mM Tris-HCL pH 8.0, 10 mM EDTA, 1%SDS, 20mg/ml sodium butyrate)
79 supplemented with phenyl methane sulfonyl fluoride and protease inhibitor cocktail (Active
80 Motif, Carlsbad, CA). DNA was sheared by sonication (Biorupter, Diagenode, Denville, NJ) into
81 200-500 bp fragments. Chromatin was pre-cleared using 30 µl protein G agarose beads (Active
82 Motif) pre-blocked with BSA per manufacturer's instructions; beads were then removed by
83 centrifugation. Chromatin was diluted with equal volume PBS, 4 µl of anti-GATA3 or isotype
84 control (Cell Signaling Technologies, Danvers, MA) added and sample incubated at 4°C with end
85 over end rotation. Next, 30 µl of pre-blocked Protein G Agarose beads was added and sample
86 incubated for 4 hours at 4°C. Beads were then sequentially washed with 1 ml each low SDS lysis
87 buffer (50mM Tris-HCL pH 8.0, 10 mM EDTA, 0.1%SDS, 20mg/ml sodium butyrate), low salt
88 buffer (10 mM Tris-HCl, pH 8, 1 mM EDTA, 50 mM NaCl), high salt buffer (50 mM Tris-HCl,
89 pH 8, 500 mM NaCl, 0.1% SDS, 0.5% Na-deoxycholate, 1% Nonidet-P40 and 1 mM EDTA) and
90 LiCl Buffer (50 mM Tris-HCl, pH 8, 250 mM LiCl, 1 mM EDTA, 1% Nonidet-P40 and 0.5% Na-
91 deoxycholate) and 1 ml TE (10 mM Tris-HCl, pH 8, 1 mM EDTA). Beads were transferred to
92 fresh tubes, centrifuged and chromatin was eluted by incubating in 100 µl elution buffer (50 mM
93 Tris-HCl, pH 8, 10 mM EDTA and 1% SDS) at 65°C with agitation. Chromatin was transferred
94 to fresh tubes and incubated with 2 µl RNase A (Qiagen, 20 mg/ml) and 6 µl 5M NaCL (Active
95 Motif) for 30 minutes at 37°C followed by 2 µl proteinase K (Active Motif, 0.2 mg/ml) at 65°C
96 for 2 hours. DNA was then purified by phenol/chloroform extraction and resuspended in nuclease

free water. Quantitative PCR was performed as described above. Primer sequences used were; FOXP3 CNS2, Forward: 5'-GGACATCACCTACCACATCC-3' Reverse: 5'-ACCACGGAGGAAGAGAAGAG-3'; β-Actin, Forward: 5'-TCCCCTCCTTTTGCGAAAA-3' Reverse: 5'- CTCCCTCCTCCTCTTCCTCAA -3'

Statistical analyses

Statistical measures, including mean values, standard deviations, Student's t-tests, Mantel–Cox tests, Mann–Whitney tests and one-way ANOVA tests, were performed using Graphpad Prism software and R. Definitions of n = values are stated in each figure legend. Where appropriate, unless otherwise stated, graphs display mean ± standard deviation.

References and Notes

1. E. Zigmond *et al.*, Ly6C hi monocytes in the inflamed colon give rise to proinflammatory effector cells and migratory antigen-presenting cells. *Immunity*. **37**, 1076–1090 (2012).
2. E. Zigmond, S. Jung, Intestinal macrophages: well educated exceptions from the rule. *Trends Immunol*. **34**, 162–168 (2013).
3. S. Z. Josefowicz, L.-F. Lu, A. Y. Rudensky, Regulatory T cells: mechanisms of differentiation and function. *Annu. Rev. Immunol.* **30**, 531–564 (2012).
4. E. Cretney, A. Kallies, S. L. Nutt, Differentiation and function of Foxp3(+) effector regulatory T cells. *Trends Immunol*. **34**, 74–80 (2013).
5. J. J. O'shea, W. E. Paul, Mechanisms Underlying Lineage Commitment and Plasticity of Helper CD4+ T Cells. *Science*. **327**, 1098–1102 (2010).
6. E. Batlle, J. Massagué, Transforming Growth Factor-β Signaling in Immunity and Cancer. *Immunity*. **50**, 924–940 (2019).
7. B. Khor *et al.*, The kinase DYRK1A reciprocally regulates the differentiation of Th17 and regulatory T cells. *Elife*. **4** (2015), doi:10.7554/eLife.05920.
8. T. B. Sundberg *et al.*, Small-molecule screening identifies inhibition of salt-inducible kinases as a therapeutic strategy to enhance immunoregulatory functions of dendritic cells. *Proc Natl Acad Sci USA* (2014), doi:10.1073/pnas.1412308111.
9. M. Chen *et al.*, Systemic Toxicity Reported for CDK8/19 Inhibitors CCT251921 and MSC2530818 Is Not Due to Target Inhibition. *Cells*. **8**, 1413 (2019).
10. R. C. Conaway, J. W. Conaway, Function and regulation of the Mediator complex. *Curr Opin Genet Dev*. **21**, 225–230 (2011).
11. S. Sato *et al.*, A set of consensus mammalian mediator subunits identified by multidimensional protein identification technology. *Mol Cell*. **14**, 685–691 (2004).

33 12. M. Malumbres, Cyclin-dependent kinases. *Genome Biol*. **15**, 122 (2014).

34 13. M. D. Galbraith *et al.*, CDK8 Kinase Activity Promotes Glycolysis. *CellReports*. **21**, 1495–
35 1506 (2017).

36 14. J. Bancerek *et al.*, CDK8 kinase phosphorylates transcription factor STAT1 to selectively
37 regulate the interferon response. *Immunity*. **38**, 250–262 (2013).

38 15. A. Lin *et al.*, Casein kinase II is a negative regulator of c-Jun DNA binding and AP-1
39 activity. *Cell*. **70**, 777–789 (1992).

40 16. C.-C. Huang *et al.*, Calcineurin-mediated dephosphorylation of c-Jun Ser-243 is required
41 for c-Jun protein stability and cell transformation. *Oncogene*. **27**, 2422–2429 (2008).

42 17. N. Taira *et al.*, DYRK2 priming phosphorylation of c-Jun and c-Myc modulates cell cycle
43 progression in human cancer cells. *J Clin Invest*. **122**, 859–872 (2012).

44 18. M. Akamatsu *et al.*, Conversion of antigen-specific effector/memory T cells into Foxp3-
45 expressing Treg cells by inhibition of CDK8/19. *Sci Immunol*. **4**, eaaw2707 (2019).

46 19. C. J. Fryer, J. B. White, K. A. Jones, Mastermind recruits CycC:CDK8 to phosphorylate
47 the Notch ICD and coordinate activation with turnover. *Mol Cell*. **16**, 509–520 (2004).

48 20. J. Shi *et al.*, Scalable synthesis of cortistatin A and related structures. *J Am Chem Soc*. **133**,
49 8014–8027 (2011).

50 21. H. E. Pelish *et al.*, Mediator kinase inhibition further activates super-enhancer-associated
51 genes in AML. *Nature*. **526**, 273–276 (2015).

52 22. L. Johannessen *et al.*, Small-molecule studies identify CDK8 as a regulator of IL-10 in
53 myeloid cells. *Nat. Chem. Biol.* **13**, 1102–1108 (2017).

54 23. A. Witalisz-Siepracka *et al.*, NK Cell-Specific CDK8 Deletion Enhances Antitumor
55 Responses. *Cancer Immunol Res*. **6**, 458–466 (2018).

56 24. E. M. Putz *et al.*, CDK8-mediated STAT1-S727 phosphorylation restrains NK cell
57 cytotoxicity and tumor surveillance. *CellReports*. **4**, 437–444 (2013).

58 25. Z. Guo, G. Wang, Y. Lv, Y. Y. Wan, J. Zheng, Inhibition of Cdk8/Cdk19 Activity
59 Promotes Treg Cell Differentiation and Suppresses Autoimmune Diseases. *Front Immunol*.
60 **10**, 775–10 (2019).
61 26. J. Martinez-Fabregas *et al.*, CDK8 Fine-Tunes IL-6 Transcriptional Activities by Limiting
62 STAT3 Resident Time at the Gene Loci. *CellReports*. **33**, 108545 (2020).
63 27. J. L. Coombes *et al.*, A functionally specialized population of mucosal CD103+ DCs
64 induces Foxp3+ regulatory T cells via a TGF-beta and retinoic acid-dependent mechanism.
65 *J Exp Med*. **204**, 1757–1764 (2007).
66 28. D. Mucida *et al.*, Reciprocal TH17 and regulatory T cell differentiation mediated by
67 retinoic acid. *Science*. **317**, 256–260 (2007).
68 29. C. M. Sun *et al.*, Small intestine lamina propria dendritic cells promote de novo generation
69 of Foxp3 T reg cells via retinoic acid. *J Exp Med*. **204**, 1775–1785 (2007).
70 30. S. Haxhinasto, D. Mathis, C. Benoist, The AKT-mTOR axis regulates de novo
71 differentiation of CD4+Foxp3+ cells. *J Exp Med*. **205**, 565–574 (2008).
72 31. J. A. Hill *et al.*, Retinoic acid enhances Foxp3 induction indirectly by relieving inhibition
73 from CD4+CD44hi Cells. *Immunity*. **29**, 758–770 (2008).
74 32. S. Sauer *et al.*, T cell receptor signaling controls Foxp3 expression via PI3K, Akt, and
75 mTOR. *Proc Natl Acad Sci USA*. **105**, 7797–7802 (2008).
76 33. J. A. Hall *et al.*, Essential role for retinoic acid in the promotion of CD4(+) T cell effector
77 responses via retinoic acid receptor alpha. *Immunity*. **34**, 435–447 (2011).
78 34. A. E. Herman, G. J. Freeman, D. Mathis, C. Benoist, CD4+CD25+ T regulatory cells
79 dependent on ICOS promote regulation of effector cells in the prediabetic lesion. *J Exp*
80 *Med*. **199**, 1479–1489 (2004).

81 35. K. V. Tarbell, S. Yamazaki, K. Olson, P. Toy, R. M. Steinman, CD25+ CD4+ T cells,
82 expanded with dendritic cells presenting a single autoantigenic peptide, suppress
83 autoimmune diabetes. *J Exp Med*. **199**, 1467–1477 (2004).
84 36. F. Powrie, M. W. Leach, S. Mauze, L. B. Caddle, R. L. Coffman, Phenotypically distinct
85 subsets of CD4+ T cells induce or protect from chronic intestinal inflammation in C. B-17
86 scid mice. *Int Immunol*. **5**, 1461–1471 (1993).
87 37. V. Valatas *et al.*, Host-dependent control of early regulatory and effector T-cell
88 differentiation underlies the genetic susceptibility of RAG2-deficient mouse strains to
89 transfer colitis. *Mucosal immunology*. **6**, 601–611 (2013).
90 38. P. M. Smith *et al.*, The microbial metabolites, short-chain fatty acids, regulate colonic Treg
91 cell homeostasis. *Science*. **341**, 569–573 (2013).
92 39. P. Kovarik *et al.*, Specificity of signaling by STAT1 depends on SH2 and C-terminal
93 domains that regulate Ser727 phosphorylation, differentially affecting specific target gene
94 expression. *EMBO J*. **20**, 91–100 (2001).
95 40. Y. Shen *et al.*, Essential role of STAT3 in postnatal survival and growth revealed by mice
96 lacking STAT3 serine 727 phosphorylation. *Mol Cell Biol*. **24**, 407–419 (2004).
97 41. L. Varinou *et al.*, Phosphorylation of the Stat1 transactivation domain is required for full-
98 fledged IFN-gamma-dependent innate immunity. *Immunity*. **19**, 793–802 (2003).
99 42. Z. Wen, Z. Zhong, J. E. Darnell, Maximal activation of transcription by Stat1 and Stat3
00 requires both tyrosine and serine phosphorylation. *Cell*. **82**, 241–250 (1995).
01 43. M. Afkarian *et al.*, T-bet is a STAT1-induced regulator of IL-12R expression in naïve
02 CD4+ T cells. *Nature Publishing Group*. **3**, 549–557 (2002).
03 44. A. A. Lighvani *et al.*, T-bet is rapidly induced by interferon-gamma in lymphoid and
04 myeloid cells. *Proc Natl Acad Sci USA*. **98**, 15137–15142 (2001).

05 45. X. O. Yang *et al.*, STAT3 regulates cytokine-mediated generation of inflammatory helper
06 T cells. *J Biol Chem*. **282**, 9358–9363 (2007).
07 46. Y. Zheng *et al.*, Genome-wide analysis of Foxp3 target genes in developing and mature
08 regulatory T cells. *Nature*. **445**, 936–940 (2007).
09 47. A. Marson *et al.*, Foxp3 occupancy and regulation of key target genes during T-cell
10 stimulation. *Nature*. **445**, 931–935 (2007).
11 48. W. Fu *et al.*, A multiply redundant genetic switch "locks in" the transcriptional signature of
12 regulatory T cells. *Nat Immunol*. **13**, 972–980 (2012).
13 49. S. Hori, T. Nomura, S. Sakaguchi, Control of regulatory T cell development by the
14 transcription factor Foxp3. *Science*. **299**, 1057–1061 (2003).
15 50. W. Zheng, R. A. Flavell, The transcription factor GATA-3 is necessary and sufficient for
16 Th2 cytokine gene expression in CD4 T cells. *Cell*. **89**, 587–596 (1997).
17 51. E. A. Wohlfert *et al.*, GATA3 controls Foxp3^{+} regulatory T cell fate during inflammation
18 in mice. *J Clin Invest*. **121**, 4503–4515 (2011).
19 52. G. Wei *et al.*, Genome-wide analyses of transcription factor GATA3-mediated gene
20 regulation in distinct T cell types. *Immunity*. **35**, 299–311 (2011).
21 53. D. Rudra *et al.*, Transcription factor Foxp3 and its protein partners form a complex
22 regulatory network. *Nat Immunol*. **13**, 1010–1019 (2012).
23 54. T. C. Fang *et al.*, Notch directly regulates Gata3 expression during T helper 2 cell
24 differentiation. *Immunity*. **27**, 100–110 (2007).
25 55. C. Mota *et al.*, Delta-like 1-mediated Notch signaling enhances the in vitro conversion of
26 human memory CD4 T cells into FOXP3-expressing regulatory T cells. *The Journal of*
27 *Immunology*. **193**, 5854–5862 (2014).
28 56. N. Joller *et al.*, Treg Cells Expressing the Coinhibitory Molecule TIGIT Selectively Inhibit
29 Proinflammatory Th1 and Th17 Cell Responses. *Immunity*. **40**, 569–581 (2014).

30 57. I. Yevshin, R. Sharipov, S. Kolmykov, Y. Kondrakhin, F. Kolpakov, GTRD: a database on
31 gene transcription regulation-2019 update. *Nucleic Acids Res.* **47**, D100–D105 (2019).
32 58. A. Subramanian *et al.*, Gene set enrichment analysis: a knowledge-based approach for
33 interpreting genome-wide expression profiles. *Proc Natl Acad Sci USA*. **102**, 15545–15550
34 (2005).
35 59. V. K. Mootha *et al.*, PGC-1alpha-responsive genes involved in oxidative phosphorylation
36 are coordinately downregulated in human diabetes. *Nat Genet*. **34**, 267–273 (2003).
37 60. M. Kitagawa, Notch signalling in the nucleus: roles of Mastermind-like (MAML)
38 transcriptional coactivators. *J Biochem*. **159**, 287–294 (2016).
39 61. Y. Wang, M. A. Su, Y. Y. Wan, An essential role of the transcription factor GATA-3 for
40 the function of regulatory T cells. *Immunity*. **35**, 337–348 (2011).
41 62. P.-Y. Mantel *et al.*, GATA3-driven Th2 responses inhibit TGF-beta1-induced FOXP3
42 expression and the formation of regulatory T cells. *PLoS Biol*. **5**, e329 (2007).
43 63. J. Wei *et al.*, Antagonistic nature of T helper 1/2 developmental programs in opposing
44 peripheral induction of Foxp3+ regulatory T cells. *Proc Natl Acad Sci USA*. **104**, 18169–
45 18174 (2007).
46 64. S. Hadjur *et al.*, IL4 blockade of inducible regulatory T cell differentiation: the role of Th2
47 cells, Gata3 and PU.1. *Immunol. Lett.* **122**, 37–43 (2009).
48 65. W. Ouyang *et al.*, Inhibition of Th1 development mediated by GATA-3 through an IL-4-
49 independent mechanism. *Immunity*. **9**, 745–755 (1998).
50 66. R. Yagi *et al.*, The Transcription Factor GATA3 Actively Represses RUNX3 Protein-
51 Regulated Production of Interferon-&gamma. *Immunity*. **32**, 507–517 (2010).
52 67. J. P. van Hamburg *et al.*, Enforced expression of GATA3 allows differentiation of IL-17-
53 producing cells, but constrains Th17-mediated pathology. *Eur J Immunol*. **38**, 2573–2586
54 (2008).

55 68. D. F. Fiorentino, M. W. Bond, T. R. Mosmann, Two types of mouse T helper cell. IV. Th2
56 clones secrete a factor that inhibits cytokine production by Th1 clones. *J Exp Med*. **170**,
57 2081–2095 (1989).
58 69. I. Menzl, A. Witalisz-Siepracka, V. Sexl, CDK8-Novel Therapeutic Opportunities.
59 *Pharmaceuticals*. **12**, 92–12 (2019).
60 70. R. Firestein *et al.*, CDK8 is a colorectal cancer oncogene that regulates beta-catenin
61 activity. *Nature*. **455**, 547–551 (2008).
62 71. P. A. Clarke *et al.*, Assessing the mechanism and therapeutic potential of modulators of the
63 human Mediator complex-associated protein kinases. *Elife*. **5** (2016),
64 doi:10.7554/eLife.20722.
65 72. J. Shi *et al.*, Stereodivergent synthesis of 17-alpha and 17-beta-alpharyl steroids:
66 application and biological evaluation of D-ring cortistatin analogues. *Angew. Chem. Int.*
67 *Ed. Engl.* **48**, 4328–4331 (2009).
68 73. D. J. Cousins, T. H. Lee, D. Z. Staynov, Cytokine Coexpression During Human Th1/Th2
69 Cell Differentiation: Direct Evidence for Coordinated Expression of Th2 Cytokines. *J*
70 *Immunol*. **169**, 2498–2506 (2002).
71 74. A. Chaudhry *et al.*, Interleukin-10 signaling in regulatory T cells is required for
72 suppression of Th17 cell-mediated inflammation. *Immunity*. **34**, 566–578 (2011).
73 75. L. W. Collison, D. A. A. Vignali, In vitro Treg suppression assays. *Methods Mol Biol*. **707**,
74 21–37 (2011).
75 76. Y. P. De Jong *et al.*, Chronic murine colitis is dependent on the CD154/CD40 pathway and
76 can be attenuated by anti-CD154 administration. *Gastroenterology*. **119**, 715–723 (2000).
77 77. C. A. Schneider, W. S. Rasband, K. W. Eliceiri, NIH Image to ImageJ: 25 years of image
78 analysis. *Nat Methods*. **9**, 671–675 (2012).

78. A. Dobin *et al.*, STAR: ultrafast universal RNA-seq aligner. *Bioinformatics*. **29**, 15–21 (2013).

79. S. Anders, P. T. Pyl, W. Huber, HTSeq--a Python framework to work with high-throughput sequencing data. *Bioinformatics*. **31**, 166–169 (2015).

80. H. Li *et al.*, The Sequence Alignment/Map format and SAMtools. *Bioinformatics*. **25**, 2078–2079 (2009).

81. H. Wickham *et al.*, Welcome to the Tidyverse. *JOSS*. **4**, 1686–6 (2019).

82. S. Durinck *et al.*, BioMart and Bioconductor: a powerful link between biological databases and microarray data analysis. *Bioinformatics*. **21**, 3439–3440 (2005).

83. D. J. McCarthy, Y. Chen, G. K. Smyth, Differential expression analysis of multifactor RNA-Seq experiments with respect to biological variation. *Nucleic Acids Res.* **40**, 4288–4297 (2012).

84. M. E. Ritchie *et al.*, limma powers differential expression analyses for RNA-sequencing and microarray studies. **43**, e47 (2015).

85. A. Liberzon *et al.*, The Molecular Signatures Database (MSigDB) hallmark gene set collection. *Cell Systems*. **1**, 417–425 (2015).

86. X. Xie *et al.*, Systematic discovery of regulatory motifs in human promoters and 3' UTRs by comparison of several mammals. *Nature*. **434**, 338–345 (2005).

87. G. Seumois *et al.*, Epigenomic analysis of primary human T cells reveals enhancers associated with TH2 memory cell differentiation and asthma susceptibility. *Nat Immunol.* **15**, 777–788 (2014).

Figure legends

Fig. 1. DCA broadly regulates differentiation of murine and human T cells. (A-C) Effect of DCA on murine naïve $CD4^+$ T cells cultured in (A) suboptimal pro-T_{reg} or -Th2 conditions (T_{reg}^{low} and $Th2^{low}$ respectively), (B) near-optimal pro-Th1 or -Th17 conditions ($Th1^{hi}$ and $Th17^{hi}$ respectively) or (C) neutral Th0 conditions (n = 4-12, x4 experiments). (D-E) Effect of DCA, all-trans retinoic acid (ATRA) and rapamycin (RAPA) on number (D) and percent (E) of T_{reg}s generated from murine (n = 9, x4 experiments) and human (n = 7-8, x3 experiments) naïve $CD4^+$ T cells cultured in T_{reg}^{low} conditions. (F) Effect of DCA on human naïve $CD4^+$ T cells cultured in $Th2^{low}$ conditions (n = 5, x2 experiments). Mann-Whitney (A-B), Kruskal-Wallis (C-E) and paired t-test (F) results, *P<0.05, ** P<0.01, *** P<0.001 ****P<0.0001.

Fig. 2. DCA describes a unique chemical immunophenotype. (A) Dose-response curves showing effect of DCA, harmine and HG-9-91-01 on murine $CD4^+$ T cells cultured in suboptimal T_{reg}^{low}, $Th2^{low}$, $Th1^{low}$ and $Th17^{low}$ conditions (n = 3-5, x3-5 experiments). Fractional maximal enhancement was determined by increase in percentage lineage-committed cells, relative to maximal cytokine-driven enhancement as previously reported (7). (B) Naive murine $CD4^+$ T cell cultures showing dose-response of the CDK8 inhibitors DCA and BRD-6989 on T_{reg} differentiation (left) and culture cellularity (right) (n = 2, x2 experiments). Harmine (HAR) is included for comparison. (C) Effect of CRISPR/Cas9-mediated deletion of CDK8, compared to mock (no guide) control, on propensity of human $CD4^+$ T cells to differentiate into T_{reg}s (left) and CDK8 expression (right). (n = 4, x2 experiments). Paired t-test (C), * P<0.05, ** P<0.01.

Fig. 3. DCA enhances differentiation of functional T_{reg}s. Suppressive function of DCA-driven T_{reg}s ($T_{reg}^{low+DCA}$, blue), compared to T_{reg}^{hi}-driven T_{reg}s (red). (A) Standard in vitro suppression assay, (B) NOD.BDC2.5 model of type 1 diabetes and (C) B10.*Rag2*$^{-/-}$ model of colitis. No-T_{reg}

28 controls shown in black. All data representative of at least 2 independent experiments (n≥4 mice
29 per cohort). Mantel-Cox (B) and Mann-Whitney (C) results, * P<0.05, ** P<0.011, *** P<0.001.
30
31 **Fig. 4. DCA regulates T cell differentiation independently of STAT1/STAT3 Ser727**
32 **phosphorylation.** (A) Effect of DCA on IL-6-induced STAT3^{Ser727} phosphorylation in resting
33 murine CD4^{+} T cells (representative of 2 independent experiments). (B-C) Effect of DCA on
34 phospho-STAT3^{Tyr705} and total STAT3 (B, n = 2, x2 experiments) and RORγt (C, n = 3, x3
35 experiments) in murine CD4^{+} T cells cultured in Th17^{hI} conditions. (D-E) Effect of DCA on Th17
36 (D) and T_{reg} (E) differentiation in *STAT3^{Ser727Ala}* naïve murine CD4^{+} T cells. (n = 8, x3
37 experiments). (F) Effect of DCA on IFNγ-induced STAT1^{Ser727} phosphorylation in resting murine
38 CD4^{+} T cells (representative of 2 independent experiments). (G-H) Effect of DCA on phospho-
39 STAT1^{Tyr705} and total STAT1 (G, n = 2, x2 experiments) and T-bet (H, n = 3, x3 experiments) in
40 murine CD4^{+} T cells cultured in Th1^{hI} conditions. (I-J) Effect of DCA on Th1 (I) and T_{reg} (J)
41 differentiation in *STAT1^{Ser727Ala}* naïve murine CD4^{+} T cells (n = 4, x2 experiments). Mann-
42 Whitney * P<0.05, ** P<0.01, *** P<0.001.
43
44 **Fig. 5. DCA drives novel early FOXP3 expression via a novel CDK8-Notch-GATA3**
45 **pathway.** (A) Timecourse of FOXP3 expression in murine CD4^{+} T cells cultured in T_{reg}^{low},
46 $T_{reg}^{low+DCA}$ and T_{reg}^{hi} conditions (n = 10, x5 experiments). (B) Effect of DCA on expression of
47 FOXP3-regulated genes in murine CD4^{+} T cells cultured for 2 days in T_{reg}^{low} conditions (n = 9, x3
48 experiments). (C) Effect of DCA on *Gata3* expression in murine (n = 3, x3 experiments) and
49 human (n = 9, x3 experiments) CD4^{+} T cells, cultured for 2 days in T_{reg}^{low} conditions. (D) Effect
50 of overexpressing GATA3, using transduction of either NGFR-T2A-GATA3 or NGFR control
51 lentivirus, on T_{reg} differentiation in human CD4^{+} T cells cultured in T_{reg}^{low} conditions (n = 12, x3
52 experiments). (E) ChIP-qPCR quantitation of how DCA treatment impacts GATA3 binding to

53 FOXP3 CNS2 in human $CD4^+$ T cells, cultured for 2 days in T_{reg}^{low} conditions (n = 3, x3
54 experiments). β-actin is included as a control locus. (F) Effect of DCA on intranuclear levels of
55 Notch intracellular domain (ICD), normalized to nuclear Lamin B1 levels, in murine and human
56 $CD4^+$ T cells stimulated for 2 hours in indicated conditions (representative of ≥2 independent
57 experiments). Mann-Whitney (B), Wilcoxan matched pair analysis (C-D) and paired t-test (E), *
58 P<0.05, ** P<0.01, *** P<0.001 ****P<0.0001.
59

60 **Acknowledgments**

61 **General**: We would like to express our deep appreciation to Anne Hocking, Karen Cerosaletti,
62 Jessica Hamerman and Daniel Campbell for helpful discussion. B10.$Rag2^{-/-}$ mice were a kind gift
63 from Dr. Brian Kelsall. We would like to acknowledge Tina Polintan for editorial assistance.
64

65 **Funding:** BK was supported by N.I.H. grant K08 DK104021.
66

67 **Author contributions:** BK, AA, RJX, PSL, VHG and TBS designed studies. AA, KGM, KJF,
68 TBS, LJ, AFS and BK conducted experiments. AA, KJF, YZ and BK analyzed data. NSG, TD,
69 YZ, DEL, IJM and ZSR provided reagents. AA and BK wrote the manuscript.
70

71 **Competing interests:** The authors have no conflicts of interest to disclose.
72

73 **Data and materials availability:** RNAseq libraries generated in this study have been made
74 available at the Gene Expression Omnibus (GEO) accession number: GSE141933
75

Figures and Tables

Fig. 1.

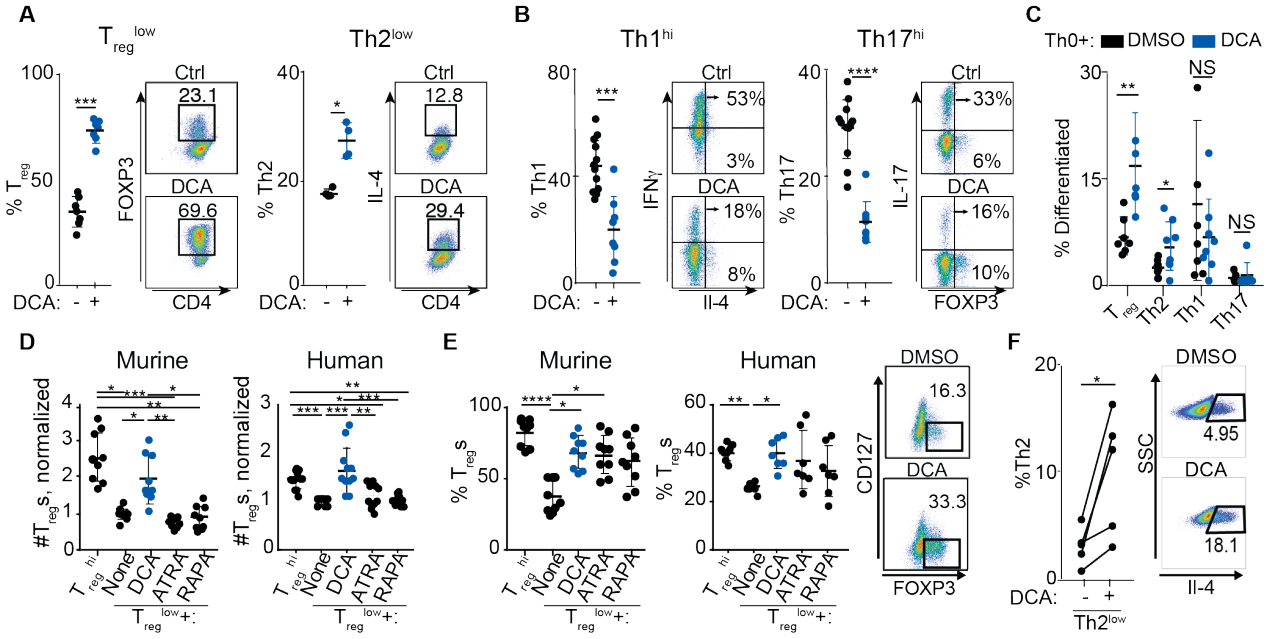

DCA broadly regulates differentiation of murine and human T cells. (A-C) Effect of DCA on murine naïve CD4$^+$ T cells cultured in (A) suboptimal pro-T_{reg} or -Th2 conditions (T_{reg}^{low} and $Th2^{low}$ respectively), (B) near-optimal pro-Th1 or -Th17 conditions ($Th1^{hi}$ and $Th17^{hi}$ respectively) or (C) neutral Th0 conditions (n = 4-12, x4 experiments). (D-E) Effect of DCA, all-trans retinoic acid (ATRA) and rapamycin (RAPA) on number (D) and percent (E) of T_{reg}s generated from murine (n = 9, x4 experiments) and human (n = 7-8, x3 experiments) naïve CD4$^+$ T cells cultured in T_{reg}^{low} conditions. (F) Effect of DCA on human naïve CD4$^+$ T cells cultured in $Th2^{low}$ conditions (n = 5, x2 experiments). Mann-Whitney (A-B), Kruskal-Wallis (C-E) and paired t-test (F) results, *P<0.05, ** P<0.01, *** P<0.001 ****P<0.0001.

93 **Fig. 2.**

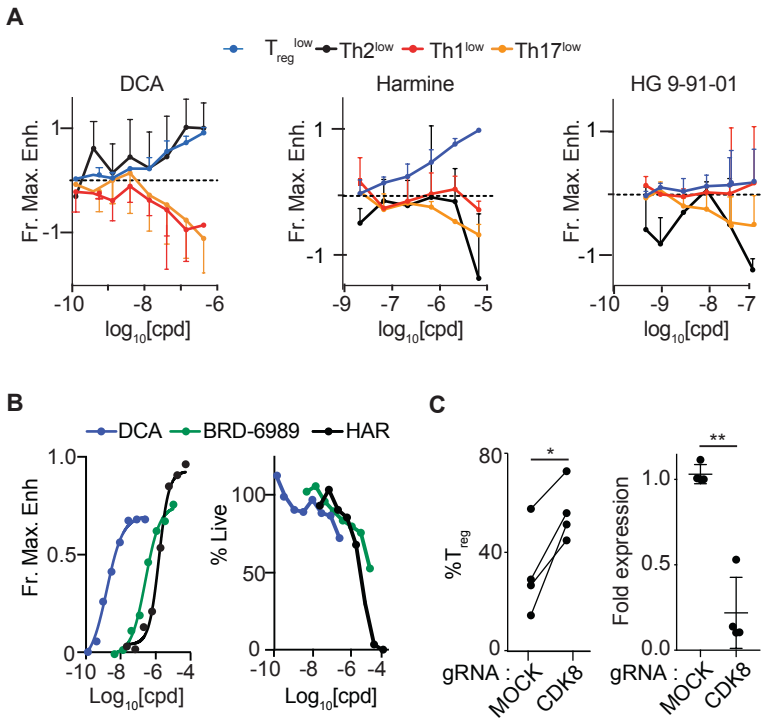

94
95

96 **DCA describes a unique chemical immunophenotype.** (A) Dose-response curves showing

97 effect of DCA, harmine and HG-9-91-01 on murine CD4$^+$ T cells cultured in suboptimal T_{reg}^{low},

98 $Th2^{low}$, $Th1^{low}$ and $Th17^{low}$ conditions (n = 3-5, x3-5 experiments). Fractional maximal

99 enhancement was determined by increase in percentage lineage-committed cells, relative to

00 maximal cytokine-driven enhancement as previously reported (7). (B) Naive murine CD4$^+$ T cell

01 cultures showing dose-response of the CDK8 inhibitors DCA and BRD-6989 on T_{reg}

02 differentiation (left) and culture cellularity (right) (n = 2, x2 experiments). Harmine (HAR) is

03 included for comparison. (C) Effect of CRISPR/Cas9-mediated deletion of CDK8, compared to

04 mock (no guide) control, on propensity of human CD4$^+$ T cells to differentiate into T_{reg}s (left) and

05 CDK8 expression (right). (n = 4, x2 experiments). Paired t-test (C), * $P<0.05$, ** $P<0.01$.

06

Fig. 3.

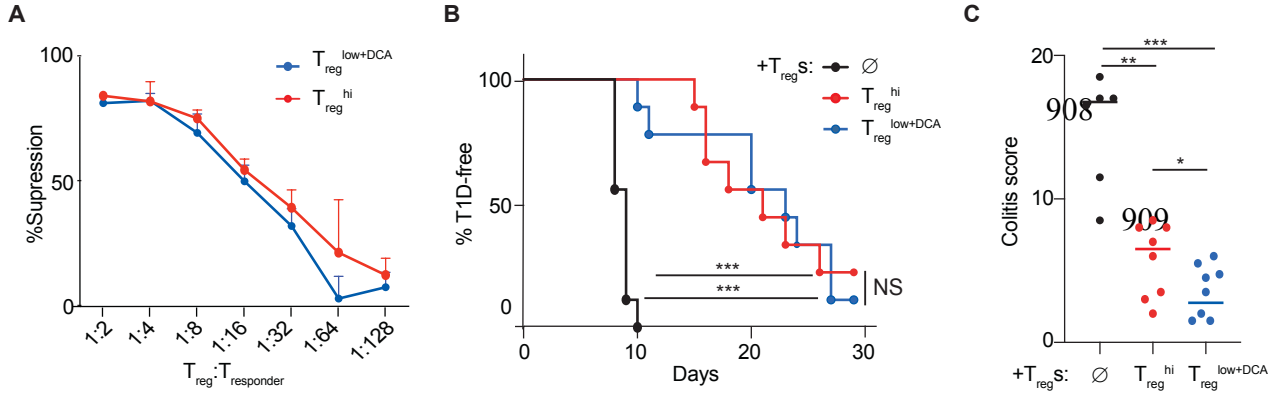

DCA enhances differentiation of functional T_{reg}s. Suppressive function of DCA-driven T_{reg}s ($T_{reg}^{low+DCA}$, blue), compared to T_{reg}^{hi}-driven T_{reg}s (red). (A) Standard in vitro suppression assay, (B) NOD.BDC2.5 model of type 1 diabetes and (C) B10.*Rag2*$^{-/-}$ model of colitis. No-T_{reg} controls shown in black. All data representative of at least 2 independent experiments (n≥4 mice per cohort). Mantel-Cox (B) and Mann-Whitney (C) results, * P<0.05, ** P<0.011, *** P<0.001.

18

19 **Fig. 4.**

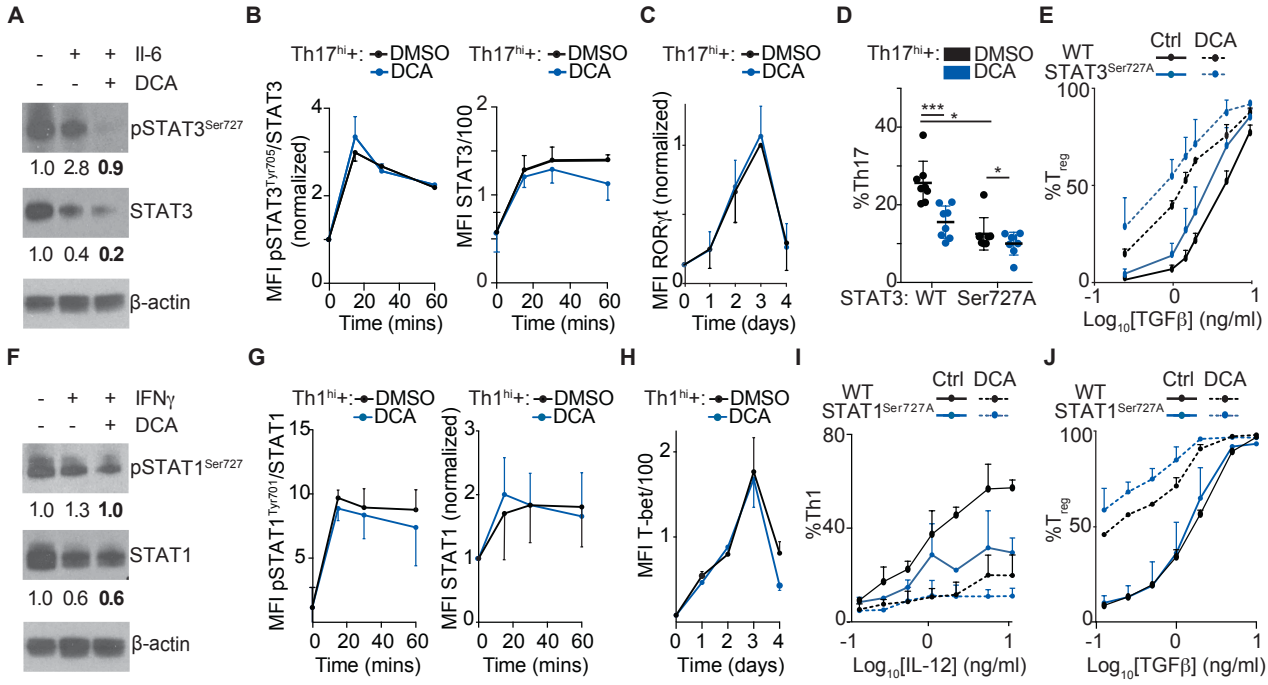

20

21

22 **DCA regulates T cell differentiation independently of STAT1/STAT3 Ser727**

23 **phosphorylation.** (A) Effect of DCA on IL-6-induced STAT3^{Ser727} phosphorylation in resting

24 murine CD4^{+} T cells (representative of 2 independent experiments). (B-C) Effect of DCA on

25 phospho-STAT3^{Tyr705} and total STAT3 (B, n = 2, x2 experiments) and RORγt (C, n = 3, x3

26 experiments) in murine CD4^{+} T cells cultured in Th17^{hI} conditions. (D-E) Effect of DCA on Th17

27 (D) and T_{reg} (E) differentiation in *STAT3^{Ser727Ala}* naïve murine CD4^{+} T cells. (n = 8, x3

28 experiments). (F) Effect of DCA on IFNγ-induced STAT1^{Ser727} phosphorylation in resting murine

29 CD4^{+} T cells (representative of 2 independent experiments). (G-H) Effect of DCA on phospho-

30 STAT1^{Tyr705} and total STAT1 (G, n = 2, x2 experiments) and T-bet (H, n = 3, x3 experiments) in

31 murine CD4^{+} T cells cultured in Th1^{hI} conditions. (I-J) Effect of DCA on Th1 (I) and T_{reg} (J)

32 differentiation in *STAT1^{Ser727Ala}* naïve murine CD4^{+} T cells (n = 4, x2 experiments). Mann-

33 Whitney * P<0.05, ** P<0.01, *** P<0.001.

34

Fig.5.

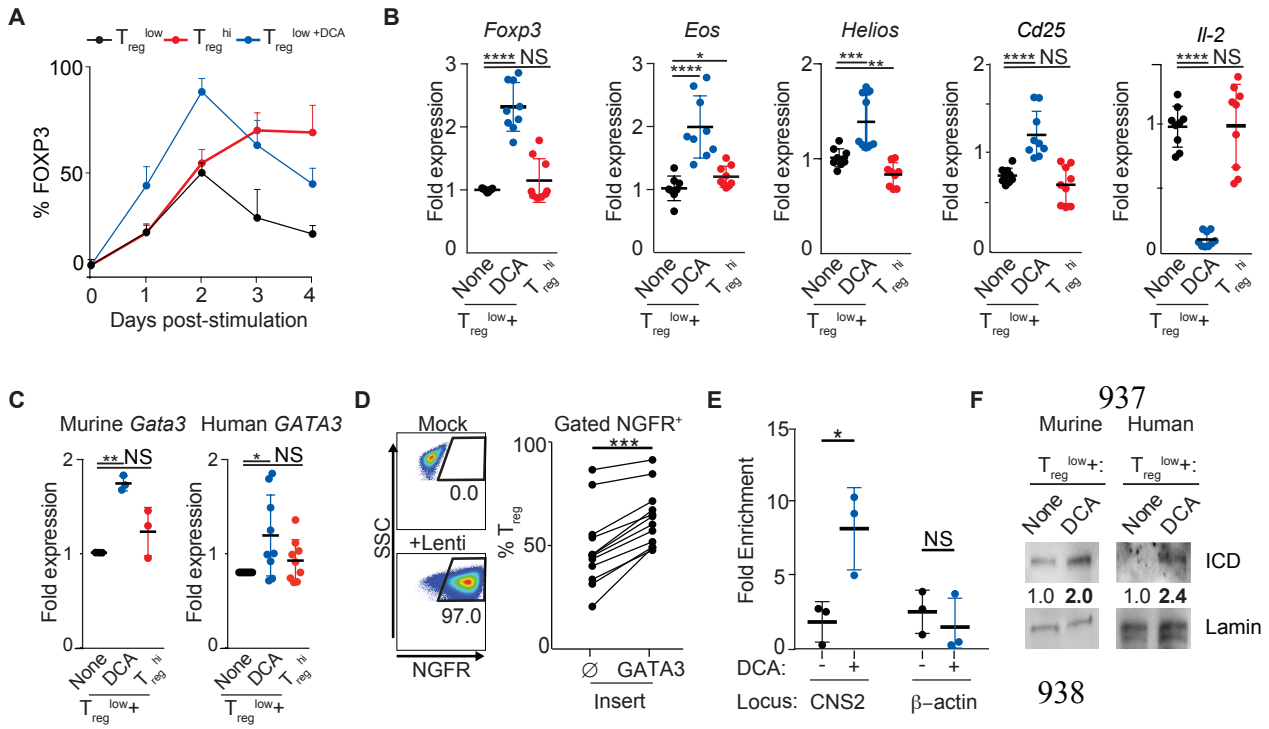

DCA drives novel early FOXP3 expression via a novel CDK8-Notch-GATA3 pathway. (A) Timecourse of FOXP3 expression in murine CD4$^+$ T cells cultured in T_{reg}^{low}, $T_{reg}^{low+DCA}$ and T_{reg}^{hi} conditions (n = 10, x5 experiments). (B) Effect of DCA on expression of FOXP3-regulated genes in murine CD4$^+$ T cells cultured for 2 days in T_{reg}^{low} conditions (n = 9, x3 experiments). (C) Effect of DCA on *Gata3* expression in murine (n = 3, x3 experiments) and human (n = 9, x3 experiments) CD4$^+$ T cells, cultured for 2 days in T_{reg}^{low} conditions. (D) Effect of overexpressing GATA3, using transduction of either NGFR-T2A-GATA3 or NGFR control lentivirus, on T_{reg} differentiation in human CD4$^+$ T cells cultured in T_{reg}^{low} conditions (n = 12, x3 experiments). (E) ChIP-qPCR quantitation of how DCA treatment impacts GATA3 binding to FOXP3 CNS2 in human CD4$^+$ T cells, cultured for 2 days in T_{reg}^{low} conditions (n = 3, x3 experiments). β-actin is included as a control locus. (F) Effect of DCA on intranuclear levels of Notch intracellular domain (ICD), normalized to nuclear Lamin B1 levels, in murine and human CD4$^+$ T cells stimulated for 2 hours in indicated conditions (representative of ≥2 independent experiments).

53 Mann-Whitney (B), Wilcoxan matched pair analysis (C-D) and paired t-test (E), * $P<0.05$, **

54 $P<0.01$, *** $P<0.001$ ****$P<0.0001$.

55